The Adipocyte-Expressed Forkhead Transcription Factor Foxc2 Regulates Metabolism Through Altered Mitochondrial Function

Martin E. Lidell,[1] Erin L. Seifert,[2] Rickard Westergren,[1] Mikael Heglind,[1] Adrienne Gowing,[2] Valentina Sukonina,[1] Zahra Arani,[1] Paula Itkonen,[3] Simonetta Wallin,[4] Fredrik Westberg,[4] Julia Fernandez-Rodriguez,[1] Markku Laakso,[3] Tommy Nilsson,[1] Xiao-Rong Peng,[4] Mary-Ellen Harper,[2] and Sven Enerbäck[1]

OBJECTIVE—Previous findings demonstrate that enhanced expression of the forkhead transcription factor Foxc2 in adipose tissue leads to a lean and insulin-sensitive phenotype. These findings prompted us to further investigate the role of Foxc2 in the regulation of genes of fundamental importance for metabolism and mitochondrial function.

RESEARCH DESIGN AND METHODS—The effects of Foxc2 on expression of genes involved in mitochondriogenesis and mitochondrial function were assessed by quantitative real-time PCR. The potential of a direct transcriptional regulation of regulated genes was tested in promoter assays, and mitochondrial morphology was investigated by electron microscopy. Mitochondrial function was tested by measuring oxygen consumption and extracellular acidification rates as well as palmitate oxidation.

RESULTS—Enhanced expression of FOXC2 in adipocytes or in cells with no endogenous Foxc2 expression induces mitochondriogenesis and an elongated mitochondrial morphology. Together with increased aerobic metabolic capacity, increased palmitate oxidation, and upregulation of genes encoding respiratory complexes and of brown fat-related genes, Foxc2 also specifically induces mitochondrial fusion genes in adipocytes. Among tested forkhead genes, Foxc2 is unique in its ability to *trans*-activate the nuclear-encoded mitochondrial transcription factor A (mtTFA/Tfam) gene—a master regulator of mitochondrial biogenesis. In human adipose tissue the expression levels of mtTFA/Tfam and of fusion genes also correlate with that of Foxc2.

CONCLUSIONS—We previously showed that a high-calorie diet and insulin induce Foxc2 in adipocytes; the current findings identify a previously unknown role for Foxc2 as an important metabo-regulator of mitochondrial morphology and metabolism.
***Diabetes* 60:427–435, 2011**

Mitochondrial number and activity are essential for many cellular functions such as ATP production through oxidative phosphorylation and biosynthesis of amino acids and lipids (1). Peroxisome proliferator–activated receptor γ coactivator-1 α (PGC1α) lies upstream of the nuclear-encoded mitochondrial transcription factor A (mtTFA/Tfam) and serves as a nutrient-sensing system that increases mitochondrial biogenesis (2). In the muscle compartment PGC1α-responsive genes linked to mitochondrial function are suppressed in humans with diabetes (3). Several investigations point toward a direct or indirect role for the mitochondria in metabolic disorders like insulin resistance and type 2 diabetes (4–7). Much research interest has focused on skeletal muscle since it accounts for ~80% of insulin-mediated glucose uptake in healthy humans. Of note, however, is the fact that the ablation of the insulin receptor in skeletal muscle does not result in overt diabetes or hyperinsulinemia (8). The adipose tissue compartment compensates for this defect by increasing its insulin-mediated glucose uptake approximately threefold (8), demonstrating clearly the capacity and overall importance of the metabolic interrelationships between adipose and muscle tissues. The capacity of adult humans to recruit mitochondria dense, energy spending brown adipose tissue (BAT) has been known for some time, as demonstrated by individuals with catecholamine-secreting tumors like phaeochromocytomas and paragangliomas; in such conditions distinct BAT depots develop (9). Lately active BAT has also been discovered in healthy adult humans (10–12), and the activation of this tissue or induction of BAT-like white adipose tissue (WAT) in humans is a highly interesting and relevant target for an antiobesity remedy.

With this in mind, and based on previous findings demonstrating that enhanced expression of the transcription factor forkhead box c2 (Foxc2) in adipose tissue leads to a lean and insulin-sensitive phenotype, which is also characterized by an enlarged BAT compartment (13), we set out to study Foxc2 regulation and effects on metabolism. We found that Foxc2 appears to induce mitochondriogenesis through activation of the *mtTFA/Tfam* promoter. Furthermore, Foxc2 induces mitochondrial fusion via activation of mitofusin 1 (*Mfn1*), mitofusin 2 (*Mfn2*), and optic atrophy 1 homolog (*Opa1*), when it is overexpressed in adipocytes and when expressed ectopically. In human adipose tissue we also found a positive

From the [1]Department of Medical and Clinical Genetics, Institute of Biomedicine, The Sahlgrenska Academy, University of Gothenburg, Gothenburg, Sweden; the [2]Department of Biochemistry, Microbiology and Immunology, Faculty of Medicine, University of Ottawa, Ottawa, Ontario, Canada; the [3]Department of Medicine, University of Kuopio and Kuopio University Hospital, Kuopio, Finland; and the [4]Bioscience Department, AstraZeneca RD, Mölndal, Sweden.

Corresponding author: Sven Enerbäck, sven.enerback@medgen.gu.se.

Received 25 March 2010 and accepted 18 November 2010.

DOI: 10.2337/db10-0409

This article contains Supplementary Data online at http://diabetes.diabetesjournals.org/lookup/suppl/doi:10.2337/db10-0409/-/DC1.

correlation between Foxc2 expression level and that of mtTFA/Tfam and Mfn1, Mfn2, and OPA1, supporting the view that this type of regulation extends to humans. This is interesting since there is growing evidence that reduction in mitochondrial fusion is an important etiological factor in development of obesity and insulin resistance (1,14,15). Based on previous findings demonstrating that Foxc2 is upregulated in response to insulin (16) and high-caloric diet (13) and on results presented herein, we propose that Foxc2 is crucial in a metabolically regulated gene circuit, allowing the adipocyte to adapt to alterations in systemic substrate availability.

RESEARCH DESIGN AND METHODS

Cell culture and transfections. 3T3-L1 cells and human embryonic kidney 293 (HEK293) cells (American *Type Culture* Collection) were cultured in Dulbecco's modified Eagle's medium (DMEM), 4.5 g/L glucose, 10% heat-inactivated FBS (Invitrogen), 100 U/mL penicillin, and 100 μg/mL streptomycin. Transfections of 3T3-L1 cells were carried out in 24-well plates using FUGENE 6 (Roche) according to the manufacturer's recommendations. In brief, reporter vectors were cotransfected with 3 ng pRL-SV40 Renilla (Promega) and an increasing amount of expression vector. Empty expression vector was added to get a final DNA amount of 1 μg per transfection. The transfection mixes were added to ~95% confluent cells, and after 17 h of culture in DMEM containing 10% FBS, differentiation was induced by supplementing the media to 5 μg/mL insulin (Sigma), 10 μmol/L dexamethasone (Sigma), and 0.5 mmol/L 3-isobutyl-1-methylxanthine (Sigma). After two days the media were replaced by DMEM containing 10% FBS and 5 μg/mL insulin. The following day cells were lysed in passive lysis buffer (Promega), and the luciferase activities were measured on a TD 20/20 luminometer (Turner Designs) using the Dual-Luciferase Reporter Assay system (Promega). The luciferase activity was normalized to the Renilla luciferase activity. The FOXC2 expression plasmid was made up by cloning FOXC2 (nt 1192–3289, GenBank: Y08223) into the pCB6$^+$ vector. Other expression vectors used were: pEVRF0-FOXF2, pcDNA3.1/GS-FOXI1, and pCDNA3-FLAG-FOXO1. For the promoter studies, PCR amplified promoter regions of *Mfn1* (nt 89726–92244 GenBank: AC130281, 2.5 kb region upstream of first exon), *Mfn2* (nt 114316–117735, GenBank: AL607066, 3.2 kb region upstream of first exon), and *mtTFA* (nt 137612–140034 GenBank: AC023170, 2.3 kb region upstream of first exon) were ligated into the pGL3-Basic (Promega). HEK293 cells overexpressing FOXC2 in a doxycycline-inducible way were created by introducing a pTRE2hyg vector (Clontech) harboring a sequence encoding FOXC2 with a COOH-terminal His-tag into 293 pTet-On cells (Clontech) and selecting for stable transfectant clones according to the manufacturers recommendations. HEK293-FOXC2-His Tet-On cells were grown in DMEM containing 4.5 g/L glucose, 10% Tet System Approved FBS (Clontech), 100 U/mL penicillin, and 100 μg/mL streptomycin. FOXC2-His expression was induced by supplementing the media with 2 μg/mL doxycycline (Clonetech). Mouse embryonic fibroblasts (MEFs) from wild-type (WT), FOXC2 transgenic (13), and Foxc2-deficient (17) embryos were isolated, grown, and differentiated into adipocytes as previously published (18). Although Foxc2-deficient mice die before or around the time of birth, they survive to E12–14, thus long enough to allow preparation of MEFs that lack Foxc2 expression.

FOXC2 adenovirus was constructed using the ViraPower Adenovirus Expression System (Invitrogen). Briefly, virus was produced by transfecting HEK293 cells with pAd/CMV/V5-DEST vector containing full-length human FOXC2 cDNA and further amplified and titered before infecting adipocytes. Human preadipocytes isolated from healthy donors with BMI under 25 (ZenBio) were seeded in 24-well plates and differentiated according to the manufacturers' recommendations. After 10 days of differentiation, cells were infected either by control adenovirus expressing ZS-green or by adenovirus expressing FOXC2 (50 multiplicity of infection/cell). After infection (72 h), total RNA was isolated using RNeasy Mini (Qiagen) and used for further studies.

Animals and cold adaptation. Cold adaptation experiments were carried out using two groups of 12-week-old C57Bl/6 mice each consisting of 10 animals (five males and five females; ethical permission, 344/08, Ethical Committee of Western Sweden). One group was kept at 4°C for 16 h, whereas the control group was kept at 20°C. WAT and BAT were dissected, and total RNA was isolated using Micro-to-Midi Total RNA Purification System (Invitrogen) according to manufacturer's instructions. Mice were fed a standard chow diet with 4% (wt/wt) fat content.

Reverse transcription and real-time PCR. Reverse transcription of 1 μg total RNA was carried out using a first strand cDNA synthesis kit for RT-PCR (Roche). Real-time PCR was performed using TaqMan Fast Universal PCR Master Mix and the 7900HT Fast Real-Time PCR System (Applied Biosystems). Primer sequences are available on request. The TaqMan assays were chosen to span an exon junction and therefore did not detect genomic DNA. For specificity, selected samples were analyzed twice with and without reverse transcriptase, and no amplification was seen in samples in the absence of reverse transcriptase.

Western blot analysis. Cell lysates were prepared using a lysis buffer (50 mmol/L Tris-HCl [pH 8.0], 1% [vol/vol] Triton X-100, 0.5% [wt/vol] sodium deoxycholate, 0.1% [wt/vol] SDS, and 150 mmol/L NaCl) containing protease inhibitors (Complete, Roche). Equal protein amounts, as assessed by bicinchoninic acid (BCA) Protein Assay (Pierce), were separated by SDS-PAGE and blotted to a polyvinylidene fluoride (PVDF) membrane (Immobilon-P, Millipore). The membrane was blocked in PBS, 0.1% (vol/vol) Tween 20, and 5% (wt/vol) milk powder, and FOXC2-His expression was determined using an anti-His tag antibody (Abcam).

Electron microscopy. Cells were processed for electron microscopy, using a double fixation protocol with osmium and tannic acid (19). Samples were dehydrated in graded ethanol series and embedded in epon 812 (Serva). After 48 h at 60°C to allow polymerization, ultra-thin sections (60 nm) were cut and mounted on grids. Samples were examined on a LEO 912 OMEGA (Zeiss) at 120 kV accelerating voltage. Digital images were obtained by a side-mount MegaView III TEM charge-coupled device (CCD) camera. Morphometric analysis of mitochondria was performed with Volocity Quantitation 4.2 (Improvision), on digital images of equal magnification based on true cross-sections of mitochondrial profiles.

Metabolic analyses. Undifferentiated MEFs were seeded (20,000 cells/well) into 24-well Seahorse XF24 plates (28 mm^2 wells) precoated with 0.4% gelatin (Invitrogen). MEFs were differentiated for 6 days, and O_2 consumption rate (OCR) and extracellular acidification rate (ECAR) were determined in an XF24 Extracellular Flux Analyzer (Seahorse Bioscience), as previously described (20). The OCR values were obtained by measuring the first 30 mmHg drop in O_2 partial pressure. ECAR values were measured as the rate of change of pH over the duration of the measurement period, usually 2 min. To obtain basal metabolic characteristics of cells, there were three measurement cycles. To assess the effects of an uncoupler and an electron transport chain inhibitor, *p*-trifluoromethoxy carbonyl cyanide phenylhydrazone (FCCP) (1 μmol/L) or antimycin A (50 nmol/L) was injected into the wells, and three more measurement cycles followed. Subsequent to metabolic analyses, MEFs were trypsinized, and total cellular protein was determined using a BCA assay.

Palmitate oxidation. Free fatty acid oxidation was assessed according to Rune et al. (21), by exposing MEF adipocytes to [^{3}H]palmitic acid and measuring the tritiated water produced. Adipocytes, cultured in 24-well plates, were washed twice with PBS and exposed to 0.25 mL of DMEM, 1 g/L glucose supplemented with 0.2% fatty acid free BSA (Sigma-Aldrich, A8806), and 0.125 μCi palmitic acid [9–10(n)-^{3}H] (5 mCi/mL, final specific activity 47.7 Ci/mmol; PerkinElmer), with or without 100 nmol/L insulin or 1 mmol/L AICAR (Sigma-Aldrich) for 5.5 h. Nonmetabolized palmitate was absorbed by incubation of 0.1 mL cell supernatant with 0.4 mL charcoal slurry (0.1 g/mL charcoal in 0.02 mol/L Tris-HCl [pH 7.5]) for 30 min. Samples were subjected to centrifugation (15 min at 16,000 *g*), 0.2 mL supernatant with tritium-bound water withdrawn, and radioactivity was determined in a liquid scintillation counter (LS7000).

Analysis of adipose tissue from humans. All subjects had normal liver, kidney, and thyroid function; no history of excessive alcohol intake; and no severe chronic diseases. Biopsies were obtained from abdominal subcutaneous adipose tissue. Subjects were 78 nondiabetic offspring of patients with type 2 diabetes. Informed consent was obtained from all subjects after the purpose and potential risks of the study were explained to them. The protocol was approved by the Ethics Committee of the University of Kuopio and was in accordance with the Helsinki Declaration. Total RNA from subcutaneous adipose tissue was isolated using TRIzol reagent (Invitrogen) and an RNeasy Mini kit (Qiagen) and transcribed to cDNA using random primers and a high-capacity cDNA archive kit (Applied Biosystems). Quantitative RT-PCRs were performed in a 7500 Real-Time PCR System (Applied Biosystems) using 6 ng (RNA equivalents) of cDNA as template, gene-specific primers and probes (information on primers and probes available upon request from Applied Biosystems). Expression levels were normalized to large ribosomal protein P0 (Hs99999902_ml, Applied Biosystems) using the standard curve method.

Statistics. All values are given as means ± SE. Student *t* test was used for statistical analyses, except in the case of the metabolic OCR and ECAR analyses, which used two-way ANOVA (mixed design) with Bonferroni post hoc tests. In the analyses after adenovirus mediated overexpression of FOXC2 in human adipocytes one-way ANOVA were used. For the analysis of gene expression in human adipose tissue Pearson correlations were calculated. A P value of less than 0.05 was considered to be significant.

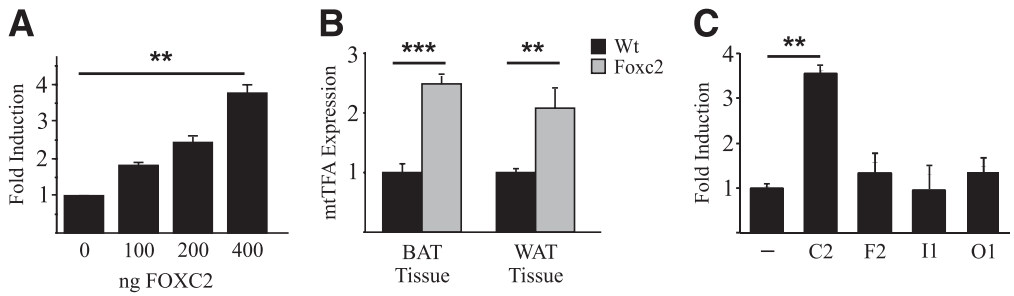

FIG. 1. Foxc2 regulates mtTFA. *A*: 3T3-L1 cells were transiently transfected with a luciferase reporter plasmid harboring an *mtTFA* promoter and an increasing amount (0–400 ng) of FOXC2 expression vector. ***P* = 0.01. *B*: Real-time PCR analysis of mtTFA mRNA expression in white adipose tissue (WAT) and brown adipose tissue (BAT) derived from Foxc2 overexpressing mice (gray bars) and WT littermates (black bars). ***P* = 0.01; ****P* = 0.001. *C*: Cotransfections in 3T3-L1 cells using *mtTFA*-promoter-luciferase reporter-construct and expression vectors for a selection of forkhead genes (*Foxc2*, *Foxf2*, *Foxi1*, and *FoxO1*). ***P* = 0.01; *n* = 3.

RESULTS

Foxc2 activates *mtTFA/Tfam* transcription in adipocytes. The findings that Foxc2 promotes formation of mitochondrial dense BAT in vivo (13) prompted us to further investigate the role of Foxc2 in the regulation of genes of fundamental importance for mitochondrial function. We made a promoter reporter construct for the nuclear-encoded mitochondrial transcription factor A (mtTFA also referred to as Tfam), which plays a crucial role in mitochondrial transcription and biogenesis (22–25).

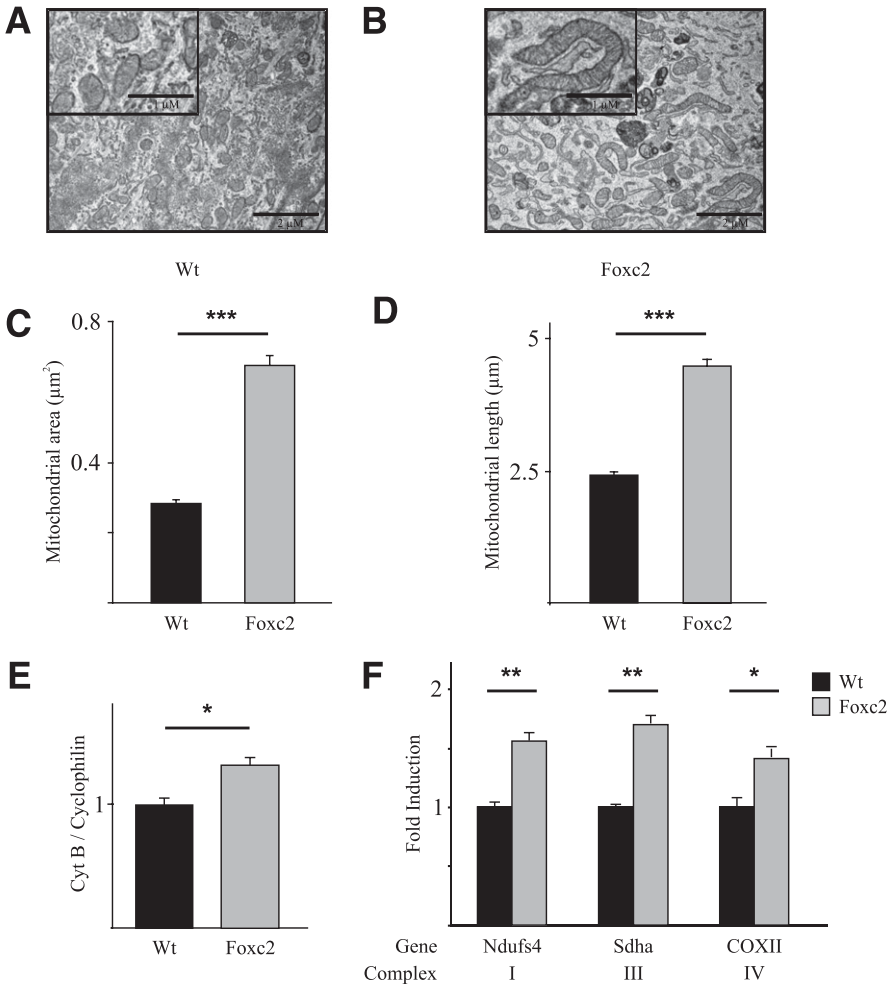

FIG. 2. MEFs with elevated Foxc2 expression have increased levels of mitochondrial DNA, elongated mitochondria, and induced expression of genes in the electron transport chain. Mitochondrial area and length measured in 150 view fields on differentiated MEFs derived from WT and Foxc2 transgenic mice (*A–D*) are shown. ****P* = 0.001. Representative electron micrographs of differentiated MEFs (*A* and *B*) are shown. Real-time PCR analysis of Cytochrome B and Cyklophilin A genomic DNA (*E*) and genes in electron transport chain complexes I (*Ndufs4*), III (*Sdha*), and IV (*COXII*) in differentiated MEFs (*F*) from Foxc2 transgenic mice (gray bars) and cells from WT littermates (black bars) is shown. **P* = 0.05; ***P* = 0.01; ****P* = 0.001; *n* = 3. Scale bar represents 2 μm (1 μm in magnified view field).

We found that in transfection experiments using 3T3-L1 adipocytes FOXC2 significantly induced mtTFA/Tfam reporter activity approximately fourfold (Fig. 1*A*). This finding was confirmed in mice having increased Foxc2 expression in adipose tissue since the steady state levels of mtTFA mRNA were elevated (Fig. 1*B*). Because the forkhead gene family has many members with similar DNA-binding domains, we were curious whether the observed mtTFA reporter activation could be extended to include other forkhead genes or whether it was a feature of some exclusiveness for Foxc2. Transfections using 3T3-L1 adipocytes demonstrate that although Foxc2, as expected, induces reporter gene activity ~3.5 times, no significant activation was observed for the forkhead genes: *Foxf2*, *Foxi1*, or *Foxo1* (Fig. 1*C*). Thus the ability to induce mtTFA appears to be restricted to Foxc2 and not a function common to all forkhead genes.

FOXC2 induces adipocyte mitochondriogenesis and altered mitochondrial structure. To evaluate the biological consequences of Foxc2 as a regulator of *mtTFA* transcription, we derived MEFs from mice transgenic for an adipose-specific *aP2-Foxc2* transgene and from WT littermates. If such MEF cells were allowed to differentiate into adipocytes, transmission electron microscopy revealed that mitochondrial area increased by over twofold in MEF adipocytes with enhanced Foxc2 levels as compared with WT MEF adipocytes (Fig. 2*A*–*C*). Moreover mitochondrial structural characteristics were affected: MEF adipocytes with enhanced Foxc2 expression have distinctly elongated mitochondria (Fig. 2*B* and *D*), which is consistent with mitochondrial fusion. This indicates that in adipocytes Foxc2 activates mitochondrial DNA synthesis and transcription as well as biogenesis and fusion. mtDNA quantifications performed using a PCR-based method showed a significant increase of mtDNA content in FOXC2 MEF adipocytes as compared with WT MEF adipocytes (Fig. 2*E*). To test whether this increase reflects a corresponding increase in genes related to mitochondrial activity we measured mRNA levels for genes encoding components of respiratory complexes I, III, and IV. Expression of the nuclear-encoded *Ndufs4* (complex I) and *Sdha* (complex II) as well as the mitochondrial-encoded *COXII* (complex IV) were significantly upregulated by ~50% (Fig. 2*F*).

Surprisingly, in the cell line HEK293 having no endogenous Foxc2 expression we found very similar effects on mitochondrial morphology when Foxc2 was conditionally expressed using a Tet-on system (Fig. 3), indicating that Foxc2 expression is sufficient to stimulate mitochondrial biogenesis and fusion. Using quantitative PCR we compared steady state mRNA levels in adipocytes having varying levels of Foxc2 and observed upregulated expression of Mfn1, Mfn2, and Opa1 in cells with higher levels of Foxc2 expression (Fig. 4*A*). Mfn1 and Mfn2 facilitate docking of mitochondria and the fusion of the mitochondrial outer membrane (26) and Opa1 is required for mitochondrial fusion and integrity of cristae (27). Interestingly, genes involved in mitochondrial fission such as fission 1 (mitochondrial outer membrane) homolog (yeast) (*Fis1*) and dynamin 1-like (*Drp1*) are not regulated in relation to Foxc2 expression levels (Fig. 4*A*). We could also show that the BAT-related genes PR domain containing 16 (*prdm16*) and deiodinase, iodothyronine, type II (*Dio2*) were upregulated in adipocytes with enhanced Foxc2 levels (Fig. 4*A*). In the MEF cells used, expression levels of uncoupling protein 1 (ucp1) remain unaffected by increased levels of Foxc2 (Fig. 4*A*). Ectopically induced Foxc2 expression in

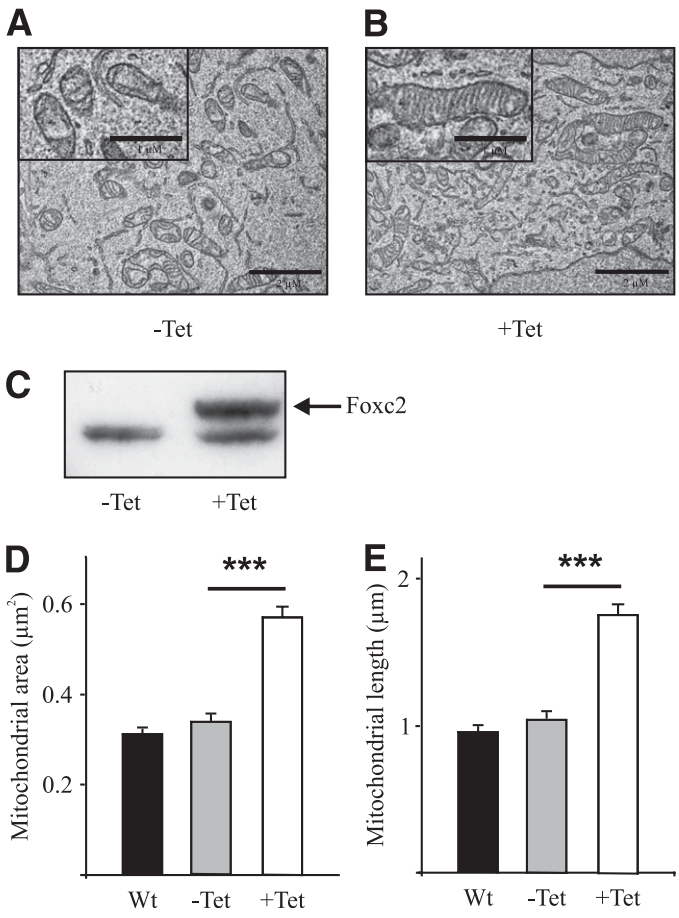

FIG. 3. Ectopic expression of Foxc2 in HEK293 cells induces mitochondrial biogenesis and fusion. Representative electron micrographs of control HEK293 cells (−Tet) (*A*) and of HEK293 cells with an induced FOXC2 expression (+Tet) (*B*) are shown. Scale bar represents 2 μm (1 μm in magnified view field). Western blot analysis (*C*) of doxycycline-induced Foxc2 expression in HEK293 cells (+Tet) and of control cells (−Tet) is shown. The upper band represents Foxc2, and the lower band is an unspecific band that serves as loading control. Mitochondrial area (*D*) and length (*E*) measured in 150 view fields on WT HEK293 cells (black bars) and on HEK293 cells presenting a doxycycline-dependent overexpression of FOXC2 before (−Tet; gray bars) and after (+Tet; white bars) doxycycline treatment are shown. ***P = 0.001.

HEK293 cells displays a close to identical gene expression pattern as compared with that in adipocytes (Fig. 4*B*), emphasizing an important Foxc2-mediated effect on mitochondrial morphology and the expression of genes involved in mitochondrial fusion and BAT-related metabolism. To verify these findings in humans we used real-time PCR to measure levels of mRNA for FOXC2, MFN1, MFN2, OPA1, PGC1β, and mtTFA/TFAM in human subcutaneous adipose tissue. We found a significant or in some cases near significant positive correlation between FOXC2 levels and MFN1 (P = 0.027), MFN2 (P = 0.058), OPA1 (P = 0.057), PGC1β (P = 0.001), and mtTFA/TFAM (P = 0.035) (Supplementary Table 1). This extends the findings described above in mice and argues in favor of a similar relationship in humans. We can also demonstrate that in transfection experiments Foxc2, in a dose-dependent fashion, transactivates both *Mfn1* and *Mfn2* promoter reporter constructs arguing for, at least in part, a direct effect of Foxc2 on these target genes (Fig. 4*C* and *D*). Using a more direct approach, we infected human adipocytes

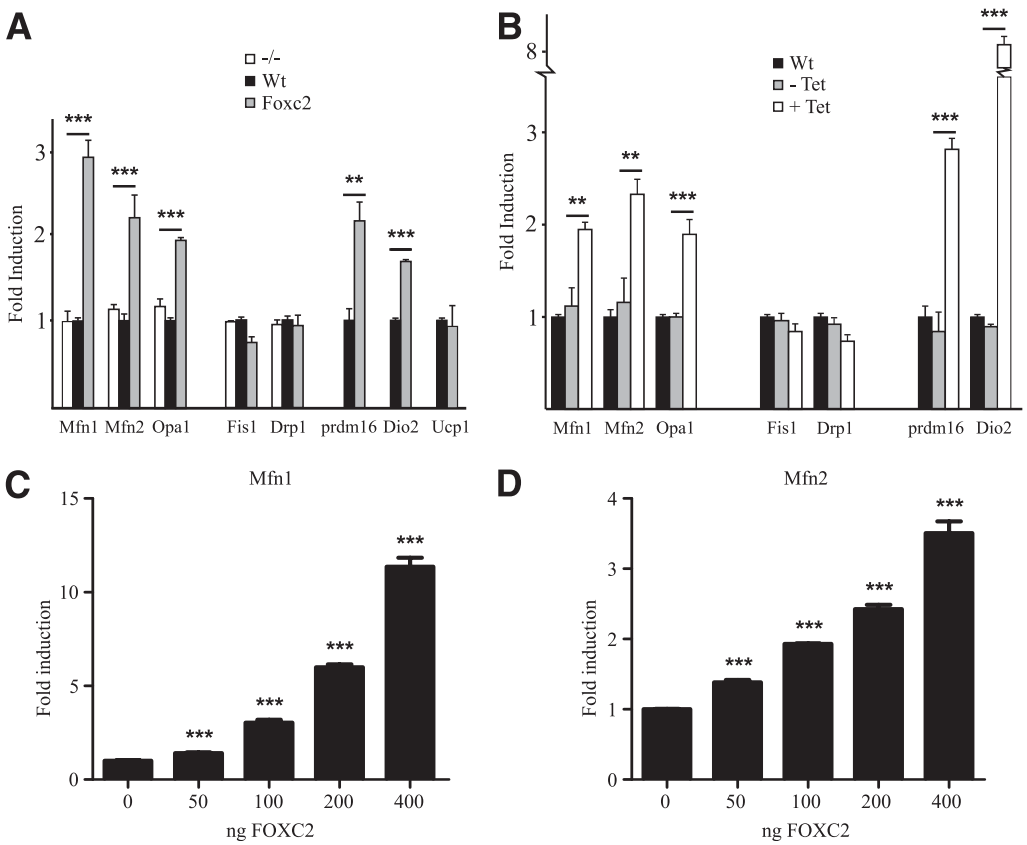

FIG. 4. Foxc2 induces expression of genes involved in mitochondrial fusion. Real-time PCR analysis of *Mfn1*, *Mfn2*, and *Opa1* (genes involved in mitochondrial fusion) and of *Fis1* and *Drp1* (genes involved in mitochondrial fission) and *Prdm16*, *Dio2*, and *Ucp1* (genes expressed in brown fat) is shown. *A*: Expression profile of MEF-derived adipocytes from mice deficient in Foxc2 expression (white bars), WT (black bars), and mice overexpressing Foxc2 (gray bars). ***P* = 0.01; ****P* = 0.001. *B*: Gene expression in WT HEK293 cells (black bars), uninduced Tet-Foxc2 HEK293 (gray bars), and induced Tet-Foxc2 HEK293 cells (white bars). ***P* = 0.01; ****P* = 0.001; *n* = 3. Transient transfections of 3T3-L1 cells with a Foxc2 expression vector together with *Mfn1* (*C*) or *Mfn2* (*D*) promoter reporter constructs show that Foxc2 induce the promoters in a dose-dependent way. ****P* = 0.001; *n* = 3.

with adenovirus expressing either ZS-green (control) or FOXC2. RNA was prepared from such adipocytes, and levels of mRNA corresponding to DIO2, PRDM16, MFN1, MFN2, and mtTFA were determined using real-time PCR. As can be deduced from Fig. 5, adipocytes overexpressing FOXC2 have significantly upregulated these genes or, in the case of mtTFA, there is a clear trend in the same direction. Thus transfection experiments (Fig. 1*A* and *C* and Fig. 4*C* and *D*), measurements of expression levels in tissues and MEF-derived adipocytes (Fig. 1*B* and Fig. 4*A*), above mentioned correlations in human adipocytes (Supplementary Table 1) as well as the result from human adipocytes transduced by a FOXC2-expressing adenovirus (Fig. 5) support the view that DIO2, PRDM16, MFN1, MFN2, and mtTFA are positively regulated by FOXC2.

Enhanced aerobic capacity in adipocytes with enhanced Foxc2 expression. To test whether these Foxc2-induced changes in mitochondrial morphology and gene expression patterns correlate with functional parameters we measured aerobic (oxygen-dependent metabolism) capacity of MEF adipocytes. Although there is no difference in oxygen consumption during unstimulated conditions, maximal uncoupled oxygen consumption was higher in adipocytes with enhanced Foxc2 expression, demonstrating a greater maximum aerobic capacity compared with WT adipocytes (Fig. 6*A*). Similar measurements were performed to assess the anaerobic metabolic capacity; here there were no differences between the two groups of adipocytes during uncoupling or basal conditions (Fig. 6*B*). We can also demonstrate an increased palmitate oxidation in MEF adipocytes with enhanced Foxc2 expression (Fig. 6*C*). Hence, an enhanced Foxc2 expression appears to positively regulate total oxidation capacity.

Foxc2 as a regulator of metabolo-regulated adaptive thermogensis. Because cold exposure is a strong inducer of facultative thermogenesis via activation of UCP1 in vivo we decided to study whether Foxc2 responds in a similar manner. WT C57Bl/6 mice were exposed to 4°C for 16 h, and subsequently RNA was prepared from BAT and WAT. Using real-time quantitative PCR methodology an expected increase in ucp1 mRNA was noted (Fig. 7*A*). Although ucp1 is induced ~10-fold, Foxc2 is repressed by factors of ~14 and ~3 in BAT and WAT, respectively (Fig. 7*B* and *C*). Hence, even though both cold adaptation and FOXC2 have been implicated as activators of UCP1 expression, they appear to act through separate mechanisms. To a large extent cold induction of ucp1 depends on activation of PGC1α (28) since deletion of PGC1α dramatically reduces cAMP-induced (29) and cold-induced (30) ucp1 activation. In this context Foxc2 is differently regulated in terms of its independence of PGC1α for cAMP-mediated induction (29) and its repression by cold in both BAT and WAT (Fig. 7*B* and *C*).

Because PGC1α and -β have been implicated as master regulators of mitochondrial biogenesis and respiration

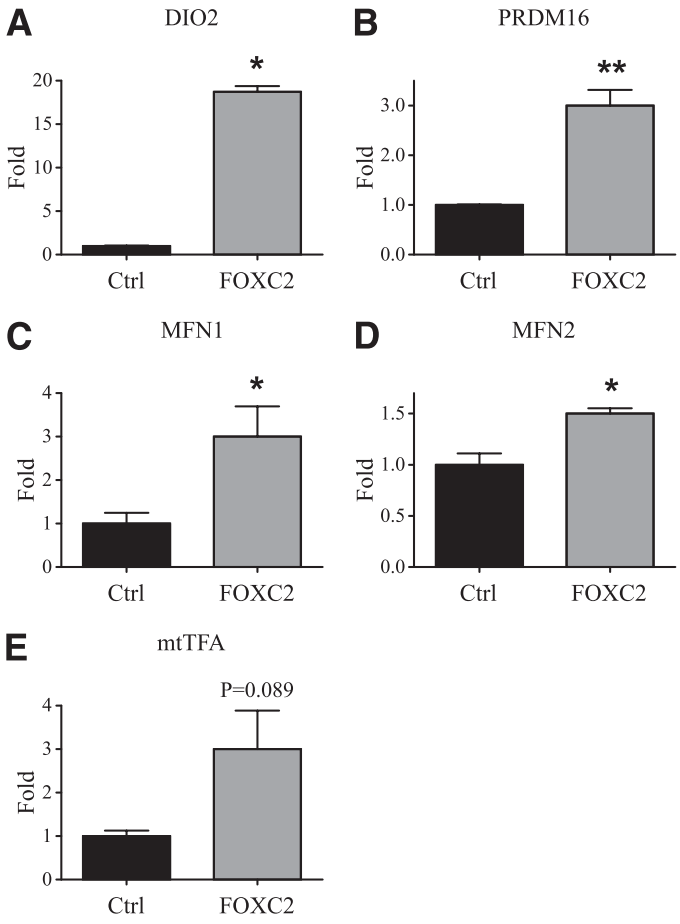

FIG. 5. Effects of an increased FOXC2 expression in human adipocytes. Quantitative real-time PCR analyses of the expression levels of DIO2 (*A*), PRDM16 (*B*), MFN1 (*C*), MFN2 (*D*), and mtTFA (*E*) in human adipocytes infected either by a control adenovirus expressing ZS-green (Ctrl) or by an adenovirus expressing FOXC2 (FOXC2) are shown. **P* = 0.05; ***P* = 0.01; *n* = 3.

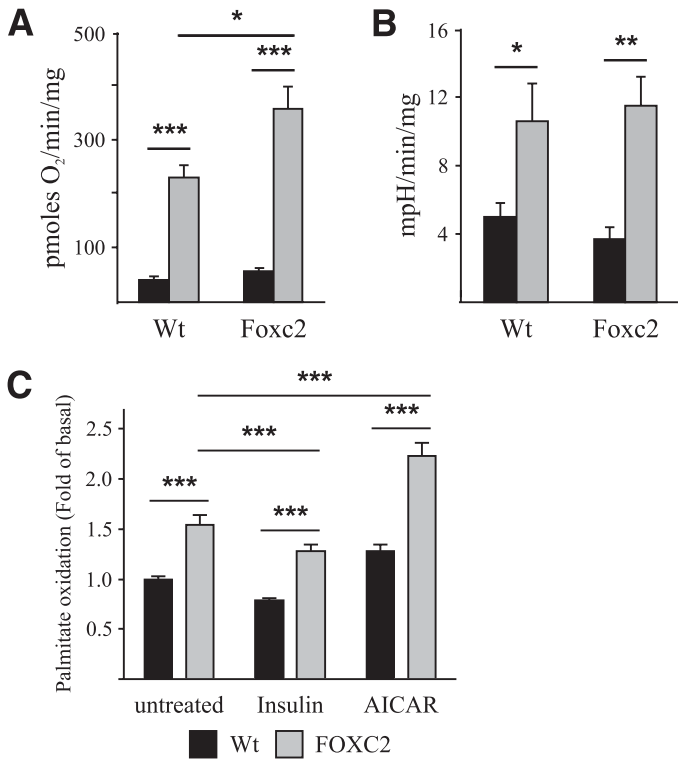

FIG. 6. Cells overexpressing Foxc2 have increased aerobic capacity and enhanced levels of palmitate oxidation. *A*: Oxygen consumption rates in MEF-derived adipocytes from WT and Foxc2 overexpressing mice. Basal rates were determined in the absence of uncoupler (black bars), whereas maximal rates were determined after the addition of uncoupler (1 μmol/L FCCP; gray bars; *n* = 4 multiwell plates/genotype). **P* = 0.05; ****P* = 0.001. *B*: Extracellular acidification rates, a surrogate measure of glycolytic activity (see RESEARCH DESIGN AND METHODS), in MEF-derived adipocytes from WT and Foxc2 overexpressing mice. Basal rates were determined in the absence of uncoupler (black bars), whereas maximal rates were determined after the addition of uncoupler (1 μmol/L FCCP; gray bars; *n* = 4 multiwell plates/genotype). **P* = 0.05; ***P* = 0.01. *C*: Palmitate oxidation was measured in MEF-derived adipocytes from WT (black bars) and FOXC2 overexpressing (gray bars) mice under basal conditions and in the presence of 100 nmol/L insulin (inhibitor of fatty acid oxidation) or 1 mmol/L AICAR (activator of AMP-activated protein kinase [AMPK]). Values are calculated as fold differences compared with palmitate oxidation under basal conditions in MEF-derived adipocytes from WT mice (*n* = six multiwell plates/genotype). ***P* = 0.01; ****P* = 0.001. As expected, insulin decreased, whereas AICAR stimulated fatty acid oxidation in a similar manner both in the adipocytes derived from WT and FOXC2 overexpressing mice. Oxidation of palmitate was higher in adipocytes with increased expression of FOXC2 compared with the WT adipocytes under basal conditions and after treatment with insulin and AMPK activator AICAR.

(29,31), we then investigated a possible interdependency between Foxc2 and these two loci in terms of regulation in adipocytes. We used MEF-derived adipocytes with varying levels of Foxc2: no expression (−/−) WT, and enhanced Foxc2 expression to score mRNA levels of PGC1α (Fig. 7*D*). In response to enhanced levels of Foxc2 there was upregulated expression of PGC1α, whereas lack of Foxc2 did not affect PGC1α expression (Fig. 7*D*). On the other hand, levels of PGC1β were repressed to approximately half of those in WT adipocytes when Foxc2 is absent. PGC1β expression was not affected by increases in Foxc2 expression (Fig. 7*D*). This is compatible with a view that cellular levels of Foxc2 mRNA influence the levels of PGC1α and -β and that Foxc2 indirectly or directly acts as an upstream regulator of PGC1α. This notion gains support from the fact that adipocytes lacking PGC1α dynamically regulate Foxc2 levels, whereas this is not the case for several other metabolically important genes, e.g., *Dio2* (29). Using the same experimental approach, we measured mtTFA mRNA levels (Fig. 7*E*) and found a profile very similar to that of PGC1α (Fig. 7*D*). Thus, although both PGC1α and mtTFA levels are upregulated in response to increased levels of Foxc2, they are not dependent on Foxc2 for basal WT levels of expression since adipocytes lacking Foxc2 have no significant difference in expression levels as compared with WT adipocytes (Fig. 7*D* and *E*).

DISCUSSION

Foxc2 expression modifies mitochondrial ultrastucture. Mitochondria in adipocytes with elevated Foxc2 expression were significantly more elongated, and there was concomitantly enhanced expression of genes known to regulate mitochondrial fusion, namely *Mfn1*, *Mfn2*, and *OPA1*, whereas genes regulating mitochondrial fission *Fis1* and *Drp1* were not regulated (Fig. 4*A*). Interestingly, these findings regarding a positive relation between Foxc2 expression and that of mtTFA/Tfam, Mfn1, Mfn2, and OPA1 can be replicated in human adipose tissue with significant or near significant correlation (Supplementary Table 1), indicating that the proposed function of Foxc2 most likely also operates in human adipose tissue. This notion is further supported by adenoviral overexpression of FOXC2 in

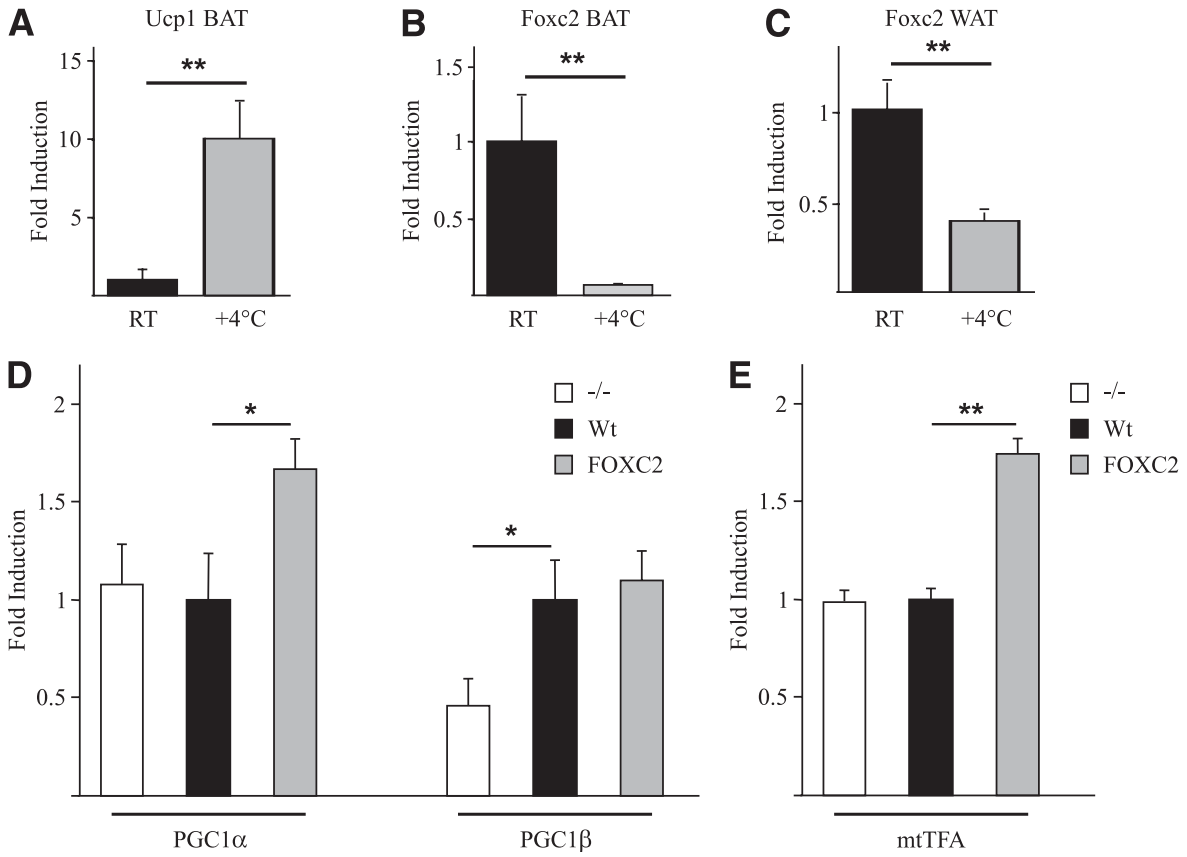

FIG. 7. Real-time PCR analysis. Measurements of Ucp1 (*A*) and Foxc2 (*B* and *C*) mRNA in WAT and BAT of WT mice, kept at room temperature (RT, black bars) or exposed to cold (+4°C for 16 h; gray bars) are shown. ***P* = 0.01. MEF-derived adipocytes overexpressing Foxc2 have induced expression of PGC1α and mtTFA. Real-time PCR analysis of PGC1α and PGC1β (*D*) and mtTFA (*E*) mRNA levels in MEF-derived adipocytes from mice deficient in Foxc2 expression (white bars), WT (black bars), and mice overexpressing Foxc2 (gray bars) is shown. **P* = 0.05; ***P* = 0.01; *n* = 3.

human adipocytes, which induce the same set of genes (Fig. 5). The ectopic expression of Foxc2 in cells that normally do not express Foxc2 was shown to be sufficient to induce mitochondrial fusion as well as some of the downstream target genes that are important in adipocytes during adaptive thermogenesis, e.g., *Dio2* and *prdm16* (Fig. 4*B*). As a functional consequence, adipocytes with enhanced Foxc2 expression have higher aerobic metabolic capacity and enhanced β-oxidation (Fig. 6). This is interesting since inhibition of fission and/or activation of fusion is found to counteract many of the disease phenotypes related to insulin resistance and diabetes (1,14,32). Moreover, it has been shown that in WAT of WT mice with enhanced life span because of caloric restriction there is an induced expression of PGC1α, mtTFA, Mfn1, and Mfn2 (33), a response very similar to what we demonstrate in adipocytes with enhanced Foxc2 expression (Figs. 1, 4, 5, and 7*D* and *E*). This emphasizes that many of the signaling pathways induced during caloric restriction also regulate energy metabolism (34), which make them interesting as potential targets for treating metabolic diseases like insulin resistance and diabetes. It also opens the possibility that even though different in some respects, cellular responses evoked by caloric restriction to some extent are similar to those activated by adaptive thermogenesis in response to, and as a possible defense against, caloric overload. Recently, it was shown that mice lacking Fsp27, a member of the Cide family of proteins, display an induction of the BAT compartment together with increased levels of Foxc2 and increase in mitochondrial size (35).

In contrast with both ucp1 and pgc1α, which are induced by cold (28,36) adipocyte, steady state levels of Foxc2 mRNA are suppressed by lowered temperature (Fig. 7*B* and *C*). Foxc2, therefore, seems to have a distinctly different role in regulation of mitochondrial function from that seen in cold-induced adaptive thermogenesis. This is interesting since UCP1 and PGC1α are indispensable components of nonshivering or thermoregulatory thermogenesis (29,30,37) and that Foxc2 activates PGC1α and mtTFA (as well as Mfn1, Mfn2, and Opa1). Supported by the results herein and the fact that Foxc2 is upregulated in response to a high-calorie diet (13) and to insulin (16), together with the fact that transgenic overexpression of Foxc2 in adipose tissue leads to expansion of the BAT tissue compartment (13), we speculate that Foxc2 plays a role in regulating a form of adaptive thermogenesis known as metaboloregulatory thermogenesis (38). This type of adaptive thermogenesis is distinct from thermoregulatory thermogenesis (which is induced by cold and dependent on cold-induced expression of PGC1α and ucp1) and is induced in rodents by cafeteria feeding, which is characterized by expanded BAT depots (39) and increased expression of brown fat-related genes like *Dio2* (40). Clearly more experiments are needed to decipher the exact relationship between metabolo- and thermoregulated adaptive heat production. However, based on the

findings presented and what is known from the literature, we would like to emphasize the fact that several features of cold-induced BAT activation such as increased BAT mass, enhanced mitochondriogensis, and activated angiogenesis to support elevated metabolism in active BAT (41) overlap with Foxc2-induced effects on BAT: increased BAT mass (13), enhanced mitochondriogensis (this article), and stimulation of angiogenesis (42), a notion that further supports the idea of two modes of BAT activation—one of cold induction and one of nutrient-regulated Foxc2 induction.

ACKNOWLEDGMENTS

This work was supported by grants to S.E. from the Swedish Research Council (Grant K2005-32BI-15324-01A), EU grants (QLK3-CT-2002-02149 and LSHM-CT-2003-503041), The Arne and IngaBritt Foundation, The Söderberg Foundation, and the Swedish Foundation for Strategic Research through the Center for Cardiovascular and Metabolic Research. Grants to M.-E.H. supporting this research include those from the Natural Sciences and Engineering Research Council and the Canadian Foundation for Innovation. E.L.S. is supported by a Canadian Diabetes Association postdoctoral fellowship.

S.W., F.W., and X.-R.P. are employed by AstraZeneca. No other potential conflicts of interest relevant to this article were reported.

M.E.L., E.L.S., R.W., M.H., A.G., V.S., Z.A., P.I., S.W., F.W., J.F.-R., M.L., and X.-R.P. researched data. M.E.L., E.L.S., R.W., M.H., A.G., V.S., Z.A., J.F.-R., T.N., M.-E.H., and S.E. contributed to discussion. M.E.L., E.L.S., R.W., A.G., V.S., J.F.-R., M.-E.H., and S.E. wrote the article. M.E.L., E.L.S, R.W., M.H., A.G., V.S., Z.A., P.I., S.W., F.W., J.F.-R., M.L., T.N., X.-R.P., M.-E.H., and S.E. reviewed and edited the article.

The authors thank Gunilla Petersson (S.E. laboratory) and Jian Xuan (M.-E.H. laboratory) for technical assistance.

REFERENCES

1. Civitarese AE, Ravussin E. Mitochondrial energetics and insulin resistance. Endocrinology 2008;149:950–954
2. Rodgers JT, Lerin C, Haas W, Gygi SP, Spiegelman BM, Puigserver P. Nutrient control of glucose homeostasis through a complex of PGC-1alpha and SIRT1. Nature 2005;434:113–118
3. Mootha VK, Lindgren CM, Eriksson KF, et al. PGC-1alpha-responsive genes involved in oxidative phosphorylation are coordinately downregulated in human diabetes. Nat Genet 2003;34:267–273
4. Björntorp P, Scherstén T, Fagerberg SE. Respiration and phosphorylation of mitochondria isolated from the skeletal muscle of diabetic and normal subjects. Diabetologia 1967;3:346–352
5. Koves TR, Ussher JR, Noland RC, et al. Mitochondrial overload and incomplete fatty acid oxidation contribute to skeletal muscle insulin resistance. Cell Metab 2008;7:45–56
6. Petersen KF, Befroy D, Dufour S, et al. Mitochondrial dysfunction in the elderly: possible role in insulin resistance. Science 2003;300:1140–1142
7. Simoneau JA, Kelley DE. Altered glycolytic and oxidative capacities of skeletal muscle contribute to insulin resistance in NIDDM. J Appl Physiol 1997;83:166–171
8. Kim JK, Michael MD, Previs SF, et al. Redistribution of substrates to adipose tissue promotes obesity in mice with selective insulin resistance in muscle. J Clin Invest 2000;105:1791–1797
9. Fukuchi K, Tatsumi M, Ishida Y, Oku N, Hatazawa J, Wahl RL. Radionuclide imaging metabolic activity of brown adipose tissue in a patient with pheochromocytoma. Exp Clin Endocrinol Diabetes 2004;112:601–603
10. Cypess AM, Lehman S, Williams G, et al. Identification and importance of brown adipose tissue in adult humans. N Engl J Med 2009;360:1509–1517
11. van Marken Lichtenbelt WD, Vanhommerig JW, Smulders NM, et al. Cold-activated brown adipose tissue in healthy men. N Engl J Med 2009;360:1500–1508
12. Virtanen KA, Lidell ME, Orava J, et al. Functional brown adipose tissue in healthy adults. N Engl J Med 2009;360:1518–1525
13. Cederberg A, Grønning LM, Ahrén B, Taskén K, Carlsson P, Enerbäck S. FOXC2 is a winged helix gene that counteracts obesity, hypertriglyceridemia, and diet-induced insulin resistance. Cell 2001;106:563–573
14. Bach D, Pich S, Soriano FX, et al. Mitofusin-2 determines mitochondrial network architecture and mitochondrial metabolism. A novel regulatory mechanism altered in obesity. J Biol Chem 2003;278:17190–17197
15. Lodi R, Tonon C, Valentino ML, et al. Deficit of in vivo mitochondrial ATP production in OPA1-related dominant optic atrophy. Ann Neurol 2004;56:719–723
16. Ridderstråle M, Carlsson E, Klannemark M, et al. FOXC2 mRNA expression and a 5′ untranslated region polymorphism of the gene are associated with insulin resistance. Diabetes 2002;51:3554–3560
17. Winnier GE, Hargett L, Hogan BL. The winged helix transcription factor MFH1 is required for proliferation and patterning of paraxial mesoderm in the mouse embryo. Genes Dev 1997;11:926–940
18. Cederberg A, Grände M, Rhedin M, Peng XR, Enerbäck S. In vitro differentiated adipocytes from a Foxc2 reporter knock-in mouse as screening tool. Transgenic Res 2009;18:889–897
19. Simionescu N, Simionescu M. Galloylglucoses of low molecular weight as mordant in electron microscopy. II. The moiety and functional groups possibly involved in the mordanting effect. J Cell Biol 1976;70:622–633
20. da-Silva WS, Harney JW, Kim BW, et al. The small polyphenolic molecule kaempferol increases cellular energy expenditure and thyroid hormone activation. Diabetes 2007;56:767–776
21. Rune A, Salehzadeh F, Szekeres F, Kühn I, Osler ME, Al-Khalili L. Evidence against a sexual dimorphism in glucose and fatty acid metabolism in skeletal muscle cultures from age-matched men and post-menopausal women. Acta Physiol (Oxf) 2009;197:207–215
22. Choi YS, Kim S, Pak YK. Mitochondrial transcription factor A (mtTFA) and diabetes. Diabetes Res Clin Pract 2001;54(Suppl. 2):S3–S9
23. Ekstrand MI, Falkenberg M, Rantanen A, et al. Mitochondrial transcription factor A regulates mtDNA copy number in mammals. Hum Mol Genet 2004;13:935–944
24. Larsson NG, Wang J, Wilhelmsson H, et al. Mitochondrial transcription factor A is necessary for mtDNA maintenance and embryogenesis in mice. Nat Genet 1998;18:231–236
25. Virbasius JV, Scarpulla RC. Activation of the human mitochondrial transcription factor A gene by nuclear respiratory factors: a potential regulatory link between nuclear and mitochondrial gene expression in organelle biogenesis. Proc Natl Acad Sci USA 1994;91:1309–1313
26. Koshiba T, Detmer SA, Kaiser JT, Chen H, McCaffery JM, Chan DC. Structural basis of mitochondrial tethering by mitofusin complexes. Science 2004;305:858–862
27. Olichon A, Baricault L, Gas N, et al. Loss of OPA1 perturbates the mitochondrial inner membrane structure and integrity, leading to cytochrome c release and apoptosis. J Biol Chem 2003;278:7743–7746
28. Puigserver P, Wu Z, Park CW, Graves R, Wright M, Spiegelman BM. A cold-inducible coactivator of nuclear receptors linked to adaptive thermogenesis. Cell 1998;92:829–839
29. Uldry M, Yang W, St-Pierre J, Lin J, Seale P, Spiegelman BM. Complementary action of the PGC-1 coactivators in mitochondrial biogenesis and brown fat differentiation. Cell Metab 2006;3:333–341
30. Lin J, Wu PH, TarrPT, et al. Defects in adaptive energy metabolism with CNS-linked hyperactivity in PGC-1alpha null mice. Cell 2004;119:121–135
31. Rohas LM, St-Pierre J, Uldry M, Jäger S, Handschin C, Spiegelman BM. A fundamental system of cellular energy homeostasis regulated by PGC-1 alpha. Proc Natl Acad Sci USA 2007;104:7933–7938
32. Yu T, Robotham JL, Yoon Y. Increased production of reactive oxygen species in hyperglycemic conditions requires dynamic change of mitochondrial morphology. Proc Natl Acad Sci USA 2006;103:2653–2658
33. Nisoli E, Tonello C, Cardile A, et al. Calorie restriction promotes mitochondrial biogenesis by inducing the expression of eNOS. Science 2005;310:314–317
34. Boily G, Seifert EL, Bevilacqua L, et al. SirT1 regulates energy metabolism and response to caloric restriction in mice. PLoS One 2008;3:e1759
35. Toh SY, Gong J, Du G, et al. Up-regulation of mitochondrial activity and acquirement of brown adipose tissue-like property in the white adipose tissue of fsp27 deficient mice. PLoS ONE 2008;3:e2890

36. Milner RE, Trayhurn P. Cold-induced changes in uncoupling protein and GDP binding sites in brown fat of ob/ob mice. Am J Physiol 1989;257:R292–R299
37. Enerbäck S, Jacobsson A, Simpson EM, et al. Mice lacking mitochondrial uncoupling protein are cold-sensitive but not obese. Nature 1997;387:90–94
38. Cannon B, Nedergaard J. Brown adipose tissue: function and physiological significance. Physiol Rev 2004;84:277–359
39. Rothwell NJ, Stock MJ. A role for brown adipose tissue in diet-induced thermogenesis. Nature 1979;281:31–35
40. Glick Z, Wu SY, Lupien J, Reggio R, Bray GA, Fisher DA. Meal-induced brown fat thermogenesis and thyroid hormone metabolism in rats. Am J Physiol 1985;249:E519–E524
41. Xue Y, Petrovic N, Cao R, et al. Hypoxia-independent angiogenesis in adipose tissues during cold acclimation. Cell Metab 2009;9:99–109
42. Xue Y, Cao R, Nilsson D, et al. FOXC2 controls Ang-2 expression and modulates angiogenesis, vascular patterning, remodeling, and functions in adipose tissue. Proc Natl Acad Sci USA 2008;105:10167–10172